Available online at www.sciencedirect.com
SCIENCE DIRECT
Catalysis Today 114 (2006) 242–247
CATALYSIS TODAY
www.elsevier.com/locate/cattod

Microcalorimetric study of sorption of water and ethanol in zeolites 3A and 5A

E. Lalik [a,*], R. Mirek [b], J. Rakoczy [b], A. Groszek [c]

[a] Institute of Catalysis and Surface Chemistry, Polish Academy of Sciences, ul. Niezapominajek 8, 30-239 Krakow, Poland
[b] Institute of Organic Chemistry and Technology, Cracow University of Technology, ul. Warszawska 24, 31-155 Krakow, Poland
[c] Microscal Ltd., 79 Southern Row, London W10 5AL, UK

Available online 17 February 2006

Abstract

Sorption of water and ethanol in zeolites 3A and 5A was investigated using gas flow-through microcalorimetry in view of finding differences in these materials performance as potential sorbents in the process of drying of ethanol. In microcalorimetric experiments, both zeolites show comparable properties for the sorption of water, but they differ profoundly in their sorption of ethanol, which was negligible small in zeolite 3A compared to zeolite 5A, in spite of the much larger enthalpy of sorption of ethanol in zeolite 3A. The difference can be explained in terms of a steric hindrance preventing the ethanol molecules from entering the narrow pores of the 3A structure, with the 5A structure remaining easily accessible for both the water and ethanol molecules alike. We propose to use a size selectivity index, defined as the ratio of sorption capacity of water and ethanol, to characterise the applicability of a zeolite as sorbent for drying of ethanol. The thermal effects of sorption of water in zeolite 3A was found to be a function of the nature of carrier gas, He or N_2, used in microcalorimetric measurements.

Keywords: Zeolite 3A; Zeolite 5A; Water; Ethanol; Heat of sorption; Flow microcalorimetry

1. Introduction

Anhydrous ethanol is widely used in the synthesis of pharmaceuticals and cosmetics, but it is also a promising fuel additive. A blend of ethanol and gasoline (gasohol) can be used as a fuel for spark-ignition engines, with an anhydrous ethanol content as low as 0.4% sufficient to improve the octane number of petrol [1–3]. Ethanol can also be used as an additive to the diesel fuels (Fuel 80) [4].

Obtaining the anhydrous ethanol, however, poses a technological problem, because of the notorious azeotrope formation at 78.15 °C and 1.013 bar, with 4.4% of water that cannot be removed by a simple distillation. The traditionally used azeotropic distillation, that involves the addition of azeotropic agent, appears to be very energy consuming and more complex methods, such as extraction, extractive distillation, and membrane separation, have attracted more interest of researchers in recent years [5–8]. On the other hand, the adsorption processes can provide a simple alternative, and as early as in 1937 [9] alumina was used as a sorbent in a pioneering research of selective adsorption of ethanol, whereas other more recent technologies use the so-called biosorbents, including corn flour, starch, and some agricultural side-products [10,11]. Increasingly, however, the zeolites seem to be winning over as the selective sorbents that are capable of ensuring industrially sustainable applications. The adsorption from liquid ethanol, produced by fermentation, leads to difficulties with the sorbent regeneration, since the traditional hot-gas-purging method causes a rapid deterioration of the sorbent bed. The turning point was the application of lowered pressure for the sorbent regeneration, following the stage of gas phase adsorption, in the so called pressure-swing-adsorption (PSA) technology, in which zeolite grains are regenerated at a low pressure, with the refluxed vapour of ethanol as a heating agent [12–15]. The advantages of PSA process include: high degree of dehydration, low energy consumption, longevity of sustainable work of the bed, the sorption performance not being affected by the fermentation side-products, and the lack of harmful emissions to the environment [13].

* Corresponding author.
E-mail address: nclalik@cyf-kr.edu.pl (E. Lalik).

0920-5861/$ – see front matter © 2006 Elsevier B.V. All rights reserved.
doi:10.1016/j.cattod.2006.01.006

Finding proper zeolite as sorbent is a prerequisite for any successful application of the adsorption technology, and the industrial practice as well as the research show that one of the most successful applications in the process of drying of ethanol is zeolite 3A [16,17]. The fact that it outperforms several other molecular sieves having similar type of crystal structure can be rationalized either in terms of a geometric hindrance leading to the so-called size-selectivity of sorption, or in terms of these structures differing in their thermodynamic affinity to the sorbate molecules. To compare both the geometric and thermodynamic aspects, we applied gas flow-through microcalorimetry, and here we report a study of the thermodynamics and the size-selectivity of sorption of water and ethanol in zeolites 3A and 5A as potential sorbents for the drying of ethanol with the PSA method. The MICROSCAL® gas flow-through microcalorimeter was used to investigate the heat of sorption as well as the kinetics of heat evolution during the adsorption and desorption of water and ethanol both at room temperature as well as at elevated temperatures ranging from 95 °C to 108 °C. We also discuss a role of different carrier gases like nitrogen or helium, which has been found to affect the thermal effects of sorption of water in zeolite 3A.

2. Experimental

2.1. Materials

The samples of zeolites 3A and 5A, which were used in sorption of both water and ethanol from helium carrier, were provided by Union Carbide, formed into cylindrical particles of average size of 4.2 mm in length and 1.8 mm in diameter. The sample of zeolite 3A Sylobead MS564 was used for a single experiment with the sorption of water from nitrogen carrier gas. For microcalorimetric measurements the material was ground, and the fraction of the grain-size from 0.5 mm to 0.35 mm was ''diluted'' with the acid washed quartz having very low surface area. The quartz-diluted material was then dried at 350 °C for 3 h prior to the experiments. In each experiment, the mass of zeolite was around 0.02 g and the mass of quartz was ca. 0.2 g. The surface area of these materials, based on the low temperature (−195 °C) adsorption of nitrogen and BET calculations, was, respectively, 15 m^2/g and 410 m^2/g for zeolites 3A and 5A.

2.2. Gas flow microcalorimetry

MICROSCAL® FMC gas flow-through microcalorimeter was used for measurements in a continuous sorption mode. The sample placed in a calorimetric cell was kept in a flow of high purity helium (or nitrogen) carrier (Polgaz, 99.999%) until reaching thermal equilibrium. The adsorption starts with replacement of pure He carrier with its mixture with water or ethanol and the end of the process is signalled by cessation of heat evolution, as well as a plateau being reached in the curve of the downstream detector, indicating no more uptake of adsorbate by the sample from the carrier. At this point, returning to the pure He-carrier flow initiated desorption from the sample. The He carrier was saturated with an adsorptive in a thermostated vessel containing either water at 17.0 °C or ethanol at 6.0 °C, at which temperatures the content of these adsorbates in the carrier gas should reach ca. 0.85 μmol/cm^3, assuming full saturation. The flow rate for both the pure and saturated carrier was 3 cm^3/min. The FMC microcalorimeter is also equipped with the downstream detector (DSD), currently a thermal conductivity detector (TCD), which makes it possible to analyse the variations in sorbate concentration in the carrier before and after the sorption, and consequently to determine the amount of material sorbed in each experiment, necessary to calculate the enthalpy of sorption.

2.3. Principle of operation of microcalorimeter

The gas flow-through microcalorimeter measures the rate of heat evolution accompanying the solid–gas interaction. The cell of microcalorimeter is placed centrally within a much larger, metal block acting as a heat sink as shown schematically (not to scale) in Fig. 1. The heat sink is large enough, first, to ensure a steady removal of the whole evolving heat, preventing its accumulation in the cell, and second, for its outer edge to be far enough away from the cell, so as not to sense the rising temperature. Hence, as the sorption is occurring within the cell, the difference of temperatures, between the close vicinity of the cell and the outermost edge of the heat sink, can be measured by a system of thermistors, appropriately located within the block (cf. Fig. 1). This temperature difference is the heat transfer driving force, and is proportional to the rate of this heat transfer by virtue of the Newton formula:

$$\dot{Q}_S = \alpha F \Delta T \tag{1}$$

whereas the rate of heat leaving the cell by heating up the gas flowing through it, can be expressed as:

$$\dot{Q}_G = \dot{m} c_p \Delta T_G \tag{2}$$

where α is the heat transfer coefficient [W/(m^2 K)], ΔT is the temperature difference between the sample and the outer edge

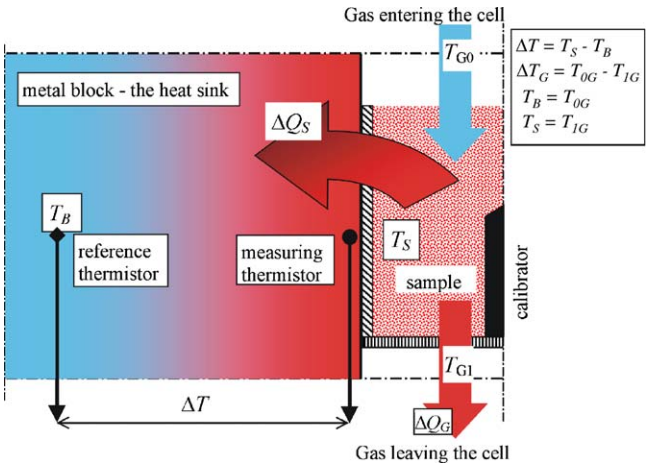

Fig. 1. Schematic representation of the heat flow in microcalorimetric measurement, shown against the partial cross-section of the calorimetric cell and the heat sink.

of metal block (heat sink), F is the geometric area of the wall of the reactor cell [m^2] (not to be confused with the surface area of the material investigated), $\dot{m}$ is the mass flow of a gas, c_p is the specific heat of the gas, and ΔT_G is the difference between the temperatures of the gas entering and leaving the cell. We can assume that the temperature of the gas on its entry to the cell T_{G0} is the same as that of the block ($T_{G0} = T_B$), and likewise that the gas heats up to the temperature of the cell ($T_{G1} = T_S$), and consequently that $\Delta T_G = \Delta T$. Therefore the total stream of heat leaving the cell both to the block and to the gas phase can be expressed as:

$$\dot{Q} = \dot{Q}_S + \dot{Q}_G = (\alpha F + \dot{m}c_p)\Delta T \quad (3)$$

It follows from the Eq. (3) that in order to calculate the rate of heat production in the process, while having measured the ΔT, one needs to know the heat transfer coefficient α, which is a very complicated function of both the physical parameters and the geometry of the system, and it would be a very tedious task to determine it separately for each new sample. This can be avoided by using the calibration factor, CF. Each experiment need to be preceded by in situ calibration procedure, in which a calibration pulse of a controlled power and duration is produced by a tiny electric coil of the calibrator located axially within the calorimetric cell (see Fig. 1), so that the calibration heat Q_{CAL} flows through the sample to the heat sink, and the resulting ΔT_{CAL} is being recorded by the system as a function of time:

$$Q_{CAL} = (\alpha F + \dot{m}c_p)\Delta T_{CAL}\tau \quad (4)$$

where τ is the electric pulse duration. Simple rearrangement yields:

$$\frac{Q_{CAL}}{\Delta T_{CAL}\tau} = \alpha F + \dot{m}c_p = CF \quad (5)$$

and the Eq. (5) defines the calibration factor CF. The heat produced on the sorption experiment can therefore be easily calculated using CF:

$$\dot{Q} = CF\Delta T \quad (6)$$

A limiting case may appear when

$$\alpha F \gg \dot{m}c_p \quad (7)$$

which means that if Eq. (7) holds, the CF might not be very sensitive to changes of neither the flow rate nor the heat capacity of the gas flowing through the cell, which both can happen as a result of the sorption process. This is an important advantage, and it has been confirmed in our experimental work.

3. Results

3.1. Sorption of water

Fig. 2 represents the calorimetric curves for adsorption and desorption of water on zeolites 3A and 5A at the high temperature. The filled areas under the calorimetric curves represent the total heat evolutions. The lower curves represent the rate of water uptake or release detected by TCD, and the filled areas under them correspond to the total amounts of sorption or desorption respectively. For both sorbents, the rate of heat evolution is highest at the initial stage of adsorption, and decrease gradually with the increasing saturation of the sample. Also the shapes of the TCD curves resemble those of the calorimetric curves, showing the highest uptake rate at the beginning of sorption. Hence for both materials, the sorption is initially most energetic.

Table 1 lists the thermal effects and the uptake of water in zeolites 3A and 5A at both the room temperature (RT) and at the higher temperature (HT). The enthalpy of adsorption/desorption is calculated as the ratio of the total heat and the uptake/release of water, respectively. The irreversible molar heat of adsorption is the ratio of irreversible heat and irreversible uptake of sorbate, calculated as a difference between the respective total heats of adsorption and desorption (irreversible heat) divided by the corresponding difference between the uptake and release of the sorbate (irreversible uptake). In both zeolites the enthalpy of adsorption of water at HT is higher than that at RT. The highest value is observed for zeolite 5A at

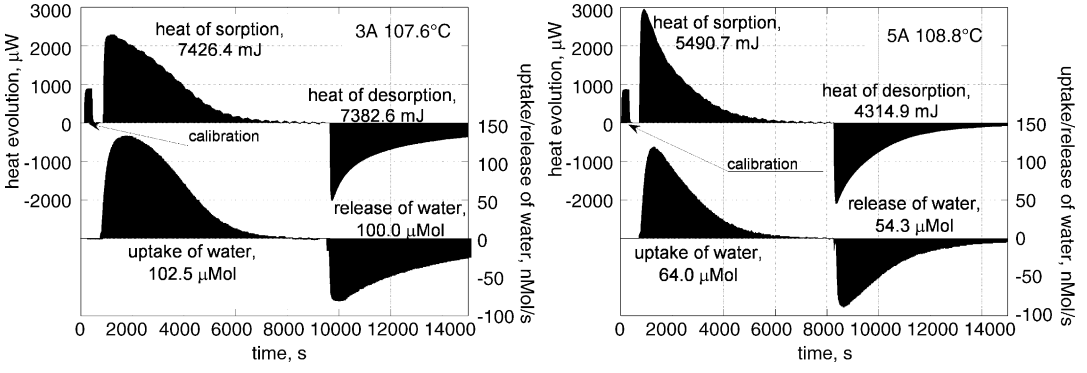

Fig. 2. The adsorption/desorption cycles of water on zeolites 3A and 5A. The upper curves represent the rate of heat evolution vs. time, so that the areas under the curves (in black) represent the total amount of heat produced on adsorption (positive) or desorption (negative). The lower curves represent the rate of uptake (adsorption) or release (desorption) of water, measured by the downstream detector, plotted as a function of time, and the areas under the curves represent the total amount of water sorbed or desorbed. See Table 1 for the calculated enthalpies of sorption.

Table 1
Sorption of water on zeolites 3A and 5A

Type of zeolite and temperature (°C)	Total heat of adsorption of H_2O (mJ)	Uptake of H_2O (μmol)	Enthalpy of adsorption of H_2O (kJ/mol)	Total heat of desorption of H_2O (mJ)	Release of H_2O on desorption (μmol)	Enthalpy of desorption of H_2O (kJ/mol)	Irreversible molar heat of adsorption (kJ/mol)
3A, RT	5612.6	98.1	57.2	2170	35.2	61.6	54.7
3A, 107.6	7426.4	102.5	72.5	7572.7	100.1	71.9	–
5A, RT	7126.8	153.0	46.6	2702.6	60.0	45.0	47.6
5A, 108.8	5490.7	64.0	85.8	4314.9	54.3	79.5	121.2
Sorption from nitrogen carrier gas							
3A, RT N_2	15584	223.7	69.7	2627	49.1	53.5	74.2

108.8 °C and is 85.8 kJ/mol. The enthalpy of adsorption at RT on the same zeolite is only 46.6 kJ/mol, very close to the heat of condensation of water, which may suggest that in this case the adsorption merely consists of condensation within the pores. At higher temperatures the formation of hydrogen bonds between the water molecules and the sorbent may result in a higher enthalpy of sorption. However, in zeolite 5A the overall amount of sorption at HT is considerably lower than that observed at RT (respectively, 64.0 μmol and 153.0 μmol). This is not the case for zeolite 3A: for this material the uptake of water turned out to be closely similar in both temperatures. The reason for the relatively low water uptake at RT in zeolite 3A may be related to the fact that helium, which is our carrier gas, can be entrapped in cavities of this zeolite to much greater extent than in zeolite 5A [18,19], particularly at lower temperatures. Hence, the water molecules seem not to be able to replace helium totally within the 3A zeolite structure at RT. This may be confirmed by our results (see the bottom row in Table 1) using nitrogen as a carrier gas for the sorption of water in zeolite 3A, under the same experimental conditions, in which case the amount of sorption of water at RT is much higher than that observed from He for approximately the same amount of sample. The irreversible molar heat of adsorption from nitrogen is 74.2 kJ/mol, in a very good agreement with the values of enthalpy of adsorption of water in zeolite 3A available in literature, 75.42 kJ/mol [20]. However, the irreversible molar heat of adsorption of water in zeolite 3A from helium at RT is only 54.7 kJ/mol (Table 1). This lower thermal effect may be explained assuming that the sorption of water proceeds via replacement of helium in zeolite 3A, and so the reduced exotherm seems to indicate the existence of a considerable endothermic effect of desorption of preadsorbed helium, which suggests that the sorption of helium in zeolite 3A is relatively strong, in agreement with Refs. [18,19].

Comparison of the adsorption and desorption values in Table 1 shows that the HT sorption of water in zeolite 3A is totally reversible. The thermal effects of adsorption and desorption are the same, within the experimental error, and also the uptake of water on sorption is the same as its release observed on desorption. Thus, in spite of relatively high enthalpy of adsorption, indicative of significant contribution from hydrogen bonding, a total desorption of water from this zeolite at HT can be achieved solely by its exposure to the water-free carrier gas, without changes in pressure or temperature.

3.2. Sorption of ethanol

Fig. 3 combines two experiments in a single graphic, in order to compare the adsorption of ethanol in zeolites 3A and 5A at HT. Clearly the uptake of ethanol in zeolite 3A (black) is very small, in fact it is negligible, in vivid contrast to zeolite 5A (grey) where a considerable amount of ethanol is sorbed. Nevertheless, the enthalpy calculated for the adsorption of ethanol in zeolite 3A is significantly larger than that in zeolite 5A (cf. Table 2). The endothermic effect visibly following the adsorption of ethanol in zeolite 5A, may possibly be related to the sorbate undergoing some undesirable catalytic reaction such as ethene formation, so that the endotherm may result from desorption of the ethene product.

Table 2 represents the thermal effects and the uptake of ethanol in zeolites 3A and 5A at both temperature ranges. The most significant thermal effect observed for zeolite 5A at 95.0 °C is also accompanied by the highest uptake of ethanol

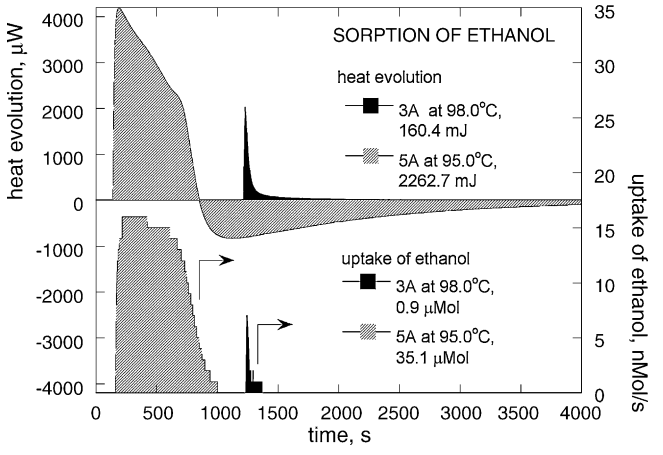

Fig. 3. Adsorption of ethanol in zeolites 3A (filled in black) and 5A (shaded). The curves representing two experiments are plotted in one figure, showing the dramatic difference in the sorption properties of the two zeolites for ethanol. The upper part shows the calorimetric curves for zeolites 3A and 5A, and the lower curves represent the corresponding uptakes of ethanol vs. time in both sorbents. The comparison of the areas under these curves demonstrates that both the thermal effects of adsorption as well as the uptakes of ethanol are much smaller for zeolite 3A. The endothermic effect visible in the upper part for the zeolite 5A results most likely from an undesired reaction, possible dehydration of ethanol to produce ethene, and may be caused by desorption of the latter. See Table 2 for enthalpies of sorption.

Table 2
Sorption of ethanol on zeolites 3A and 5A

Type of zeolite and temperature (°C)	Total heat of adsorption of ethanol (mJ)	Uptake of ethanol (μmol)	Enthalpy of adsorption of ethanol (kj/mol)	Total heat of desorption of ethanol (mJ)	Release of ethanol on desorption (μmol)	Enthalpy of desorption of ethanol (kJ/mol)	Irreversible molar heat of adsorption (kJ/mol)
3A, RT	180.7	1.5	120.5	57.1	0.4	142.7	112.4
3A, 98.0	160.4	0.9	178.2	58.2	0.5	116.4	255.5
5A, RT	727.8	14.9	48.8	195.5	4.8	40.7	52.7
5A, 95.0	2262 (exo)	35.1	63.8 (exo)	429.7	8.1	53.0	67.9

(35.1 μmol). However the enthalpy of adsorption calculated as the ratio of these two values must be considered with caution, as the heat evolution may be partly affected by the undesired catalytic dehydration of ethanol. An additional source of uncertainty lays in the minute amount of ethanol sorbed in zeolite 3A, making the values of enthalpy calculated for this material very prone to the systematic error of the downstream detector TCD.

3.3. Differential heat of sorption

The numerical differentiation of the calorimetric curve, with respect to the uptake of sorbate, yields a new curve, the so-called differential heat of sorption (DHS) curve. Plotted as a function of surface coverage, the DHS curves make it possible to compare the kinetics of sorption for different experiments. Fig. 4 shows the DHS curves for adsorption of water in both zeolites at both temperatures. It can be observed that the initially large heat of adsorption decreases with the progress of the process, reaching eventually an approximately constant rate of heat evolution of ca. 60 kJ/mol, with a single exception for the sorption on zeolite 5A at RT, notably lacking the initial period of higher energy evolution. This may indicate that the chemical bonding of the water molecules occurs only during the initial stage of sorption, causing the higher rate of heat evolution, whereas the condensation of water within the structure of zeolites is mainly responsible for the stable thermal effect at the further stage of sorption. In agreement with this, we note that the enthalpy of sorption in 5A at RT is simply equal to the heat of condensation of water, whereas for the cases featuring the differential heats initially higher, their corresponding enthalpies of sorption surpass the heat of condensation (see Table 1). Our DHS curves are comparable to those obtained by other researchers for 3A and other zeolites [21], in that in most cases, after somehow different initial periods, for the higher surface coverage the heat evolution eventually stabilizes at ca 60 kJ/mol.

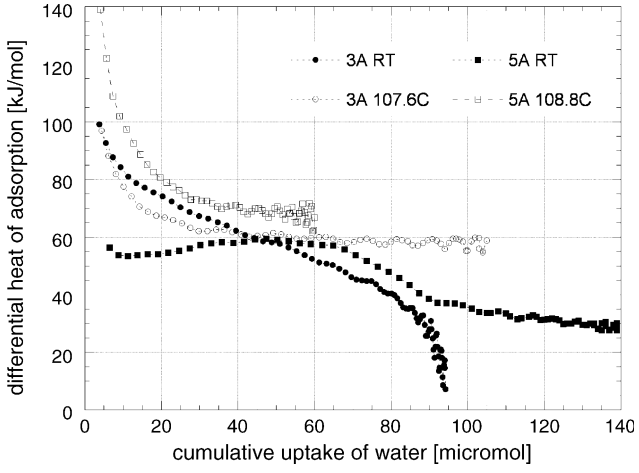

Fig. 4. Differential heats of adsorption of water for zeolites 3A and 5A.

4. Discussion

The total reversibility of sorption of water from helium in zeolite 3A at HT, revealed by microcalorimetric experiments, gives the material a clear technological advantage over its potential 5A rival, effecting an easy regeneration of a sorbent bed, solely by means of reducing partial pressure of water in the gas phase. However, apart from this difference in kinetics of sorption, both the uptakes of water as well as the enthalpies of sorption observed for both zeolites are comparable. Ethanol, in contrast, shows much more significant differences. The amount of ethanol sorbed from helium in zeolite 5A is larger by several orders of magnitude than that sorbed from He in zeolite 3A. However, the large sorption in zeolite 5A is accompanied by the molar heat of adsorption significantly lower than that observed for zeolite 3A, in spite of the minute sorption in the latter material. This suggests that the minuscule adsorption cannot result from a weak affinity of zeolite 3A to ethanol; in fact the large enthalpy seems to be indicative of an affinity being relatively strong. The reason, therefore, for the low sorption capacity of zeolite 3A is confirmed to be related to a steric hindrance. The pore size in the structures of zeolite 3A is 0.38 nm [22], that is, much less than the critical diameter of an ethanol molecule, which is 0.44 nm [23]. The ethanol molecules cannot penetrate the 3A structure. Thus, the surface effectively available for ethanol is very limited, as the adsorption can only take place on the external surface, usually being a small fraction of the total surface of a porous material. On the other hand, the pore size in the 5A structure is 0.49 nm [24], which is large enough to accommodate the ethanol molecules, making both the internal and the external surface readily accessible to the ethanol sorption. Thus, the total surface exposed to ethanol adsorption in zeolite 5A is much larger than that available in zeolite 3A.

A similar effect, of the surface being only partly accessible to a sorbate due to a steric hindrance, could be noted for the BET surface area measurements carried out with nitrogen

Table 3
Saturation values reached in dynamic sorption capacity measurements for water and ethanol, and the size-selectivity index (see text) for zeolites 3A and 5A at the room temperature and at the higher temperature range

Type of zeolite and temperature range (°C)	Sorption capacity of water, S_{water} (mol/kg)	Sorption capacity of ethanol, $S_{ethanol}$ (mol/kg)	Size-selectivity index (SSI)
3A, RT	4.6	0.075	61.3
3A, 98.0–107.6	4.9	0.044	111.4
5A, RT	7.6	0.74	10.3
5A, 95.0–108.8	3.0	1.7	1.8

adsorption at −195 °C. The resulting surface area for zeolite 3A was as small as 15 m^2/g, whereas for zeolite 5A a more ''reasonable'' result of 410 m^2/g was obtained. The former result seems unusually low for zeolites, but can be rationalized by noting that the relatively large N_2 molecules do not penetrate the pores of zeolite 3A. We note that the ratio of the two BET surface areas being approximately 15/410 = 0.037 is relatively close to the ratio of sorption capacities of ethanol in zeolites 3A and 5A, which are 0.041 and 0.025 at RT and HT, respectively. For water sorption, no steric hindrance should be expected in neither of zeolites tested, since the 0.26 nm critical diameter of water makes the molecules penetrate easily the pores of the 5A and 3A structure alike.

4.1. Size-selectivity index

A ratio of the sorption capacities of water and ethanol in a zeolite at the same temperature can be used as a measure of its drying capability. The so defined size-selectivity index (SSI) can be expressed as follows:

$$\mathrm{SSI} = \frac{S_{\mathrm{water}}}{S_{\mathrm{ethanol}}} \tag{8}$$

where S_{water} and $S_{ethanol}$ are the amounts of water and ethanol adsorption, respectively. Table 3 shows that the SSI is higher for zeolite 3A at both RT and HT (61.3 and 111.4, respectively). The lack of size-selective sorption on in zeolite 5A is signalled by much lower value of SSI.

5. Conclusions

Sorption of water from helium in zeolite 3A at HT (around 100 °C) is totally reversible. The same sorption capacities of water in zeolite 3A are observed at both RT and HT, possibly due to the effect of the structure of zeolite 3A being partially blocked by encapsulated atoms of the helium carrier that cannot be displaced by water at RT. Compared to the heat of sorption from nitrogen, the heat of sorption of water from helium at RT is significantly reduced, presumably by the endothermic effect of desorption of preadsorbed helium atoms, indicative of a possibility of strong adsorption of He in zeolite 3A, also reported in Refs. [18,19]. This strong adsorption of helium in 3A zeolite may help to improve the water desorption kinetics, which seems relevant to industrial practice.

Generally speaking, this work confirms that the use of flow-through adsorption methodology, and the associated heat of adsorption measurements, can reveal novel aspects of selective adsorption phenomena.

References

[1] L. Kornblit, A. Marchut, Nafta-Gaz 5 (1996) 217.
[2] J. Jakóbiec, A. Marchut, Nafta-Gaz 6 (2000) 341.
[3] L. Richard, P.E. Bechtold, Alternative Fuels Guidebook, SAE Inc., Warrendale, 1997.
[4] P. Satge de Caro, Z. Mouloungui, G. Vaitilingom, J.Ch. Berge, Fuel 80 (2001) 565.
[5] Y. Morigami, et al. Sep. Purif. Technol. 25 (2001) 251.
[6] D. Dhah, et al. J. Membr. Sci. 179 (2000) 185.
[7] M. Nomura, T. Bin, S. Nakao, Sep. Purif. Technol. 27 (2002) 59.
[8] Fu-Ming, R.H. Pahl, Dehydration of alcohol with extractive distillation, US Patent 4,559,109, 1985.
[9] R.B. Derr, Method of drying alcohol, US Patent 2,137,605, 1937.
[10] J.W. Priegnitz, Process for the separation of water from ethanol, US Patent 4,333,740, 1982.
[11] M.R. Ladish, G.T. Tsao, Vapour phase dehydration of aqueous alcohol mixtures, US Patent 4,345,973, 1982.
[12] W.K. Teo, D.M. Ruthven, Ind. Eng. Chem. Process Des. Dev. 25 (1986) 17.
[13] K. Kupiec, L. Zielinski, D. Jurczak, Inżynieria i Aparatura Chemiczna 5 (2002) 14.
[14] W.F. Ginder, Method of removing water from ethanol, US Patent 4,407,662, 1983.
[15] D.M. Ruthven, S. Farooq, K.S. Knaebel, Pressure Swing Adsorption, VCH Publishers Inc., 1994.
[16] B. Sowerby, B.D. Crittenden, Gas Sep. Purif. 2 (1988) 77.
[17] M.J. Carmo, J.C. Gubulin, Adsorption 8 (2002) 235.
[18] Y. Finkelstein, A. Saig, A. Danon, J.E. Koresh, J. Phys. Chem. B 107 (2003) 9170.
[19] A. Saig, Y. Finkelstein, A. Danon, J.E. Koresh, J. Phys. Chem. B 107 (2003) 13414.
[20] N. Kielcew, Podstawy techniki adsorpcyjnej, WNT, Warszawa, 1980, p. 167.
[21] R.M. Barrer, P.J. Cram, Adv. Chem. Ser. 102 (1971) 105.
[22] A. Ciembroniewicz, Kinetyka adsorpcji gazów w zeolitach i sitach cząsteczkowych typu A, Zeszyty Naukowe AGH, Kraków, 1993.
[23] S.M. Ben-Shebil, Chem. Eng. J. 74 (1999) 197.
[24] D.W. Breck, Zeolite Molecular Sieves, John Wiley & Sons, 1974.